⌘ *Author's Choice*

THE JOURNAL OF BIOLOGICAL CHEMISTRY VOL. 284, NO. 32, pp. 21446–21457, August 7, 2009

Human Heart Mitochondrial DNA Is Organized in Complex Catenated Networks Containing Abundant Four-way Junctions and Replication Forks*[S]

Received for publication, March 12, 2009, and in revised form, May 4, 2009 Published, JBC Papers in Press, June 12, 2009, DOI 10.1074/jbc.M109.016600

Jaakko L. O. Pohjoismäki[‡§¶], Steffi Goffart[‡§], Henna Tyynismaa[‖], Smaranda Willcox[**], Tomomi Ide[‡‡], Dongchon Kang[§§], Anu Suomalainen[‖], Pekka J. Karhunen[¶], Jack D. Griffith[**], Ian J. Holt[¶¶], and Howard T. Jacobs[‡§1]

*From the [‡]Institute of Medical Technology, [§]Tampere University Hospital, and [¶]Department of Forensic Medicine, University of Tampere, FI-33014 University of Tampere, Finland, [‖]Department of Neurology, Helsinki University Central Hospital and Research Programme of Molecular Neurology, Biomedicum-Helsinki, University of Helsinki, FI-00290 Helsinki, Finland, **Lineberger Comprehensive Cancer Center, University of North Carolina, Chapel Hill, North Carolina 27599-7295, Departments of [‡‡]Cardiovascular Medicine and [§§]Clinical Chemistry and Laboratory Medicine, Kyushu University Graduate School of Medical Sciences, Fukuoka 812-8582, Japan, and [¶¶]Medical Research Council (MRC)-Mitochondrial Biology Unit, Wellcome Trust/MRC Building, Hills Road, Cambridge CB2 OXY, United Kingdom*

Analysis of human heart mitochondrial DNA (mtDNA) by electron microscopy and agarose gel electrophoresis revealed a complete absence of the θ-type replication intermediates seen abundantly in mtDNA from all other tissues. Instead only Y- and X-junctional forms were detected after restriction digestion. Uncut heart mtDNA was organized in tangled complexes of up to 20 or more genome equivalents, which could be resolved to genomic monomers, dimers, and linear fragments by treatment with the decatenating enzyme topoisomerase IV plus the cruciform-cutting T7 endonuclease I. Human and mouse brain also contained a population of such mtDNA forms, which were absent, however, from mouse, rabbit, or pig heart. Overexpression in transgenic mice of two proteins involved in mtDNA replication, namely human mitochondrial transcription factor A or the mouse Twinkle DNA helicase, generated abundant four-way junctions in mtDNA of heart, brain, and skeletal muscle. The organization of mtDNA of human heart as well as of mouse and human brain in complex junctional networks replicating via a presumed non-θ mechanism is unprecedented in mammals.

The structure and organization of mitochondrial DNA (mtDNA)[2] vary considerably in different organisms (1, 2). The complexity and diversity of plant and fungal mitochondrial genomes is contrasted by the apparent simplicity of mtDNA organization in metazoans. mtDNA replication also differs between taxa: in protists, fungi, and plants documented mechanisms include conventional θ replication (3), rolling circle replication (4–6), and recombination-dependent replication (7, 8). Some mitochondrial plasmids also utilize reverse transcription (9).

In animals, where the mitochondrial genome is generally a compact circular molecule, conventional θ replication was first documented in 1968 by electron microscopy (10). Subsequent to this, a novel mechanism of DNA replication was proposed based on further electron microscopy and end mapping (11–14). This strand displacement model envisaged a single unidirectional origin for synthesis of the leading (heavy) strand (O_H), which proceeds approximately two-thirds of the way around the genome until the lagging (light) strand origin (O_L) is exposed on the displaced parental heavy strand. In this model the two strands are synthesized asynchronously and strand-continuously, obviating the need for Okazaki fragments.

The validity of this model has recently been questioned based on findings from two-dimensional agarose gel electrophoresis (AGE), ligation-mediated PCR and nascent strand analysis (15–20). These studies revealed evidence for fully duplex θ replication intermediates indicative of strand-coupled replication. However, many intermediates had extensive segments of RNA incorporated throughout the lagging strand (denoted RITOLS). The location of the replication origin also appeared to vary with some initiation events occurring bidirectionally at positions other than O_H but with O_H acting as a replication terminus.

Molecular recombination initiated by double strand breaks is now recognized as a universal and indispensable adjunct to DNA replication. It permits DNA replication to recover from fork collapse (21). Stalled replication forks regress to form Holliday junction structures both in mammalian cells (22) and bacteria (23–25). These are then processed to restart replication via the action of junctional resolvases and other components of the recombination machinery (25–28). Recombination can also initiate DNA replication in some systems, notably bacterio-

* This work was supported, in whole or in part, by National Institutes of Health Grant GM31819. This work was also supported by the Academy of Finland, Sigrid Juselius Foundation, Tampere University Hospital Medical Research Fund, Universities of Tampere and Helsinki, Yrjö Jahnsson Foundation, Elli and Elvi Oksanen Fund of the Pirkanmaa Fund under the auspices of the Finnish Cultural Foundation, Finnish Foundation for Cardiovascular Research, Helsinki Biomedical Graduate School, European Union (EUMITOCOMBAT project), and the United Kingdom Medical Research Council.

⌘ *Author's Choice*—Final version full access.

[S] The on-line version of this article (available at http://www.jbc.org) contains supplemental Figs. 1–4 and Table 1.

[1] To whom correspondence should be addressed: Inst. of Medical Technology and Tampere University Hospital, FI-33014 University of Tampere, Finland. Tel.: 358-3-35517731; Fax: 358-3-35517710; E-mail: howard.t.jacobs@uta.fi.

[2] The abbreviations used are: mtDNA, mitochondrial DNA; O_H, origin for synthesis of the leading (heavy) strand; O_L, lagging (light) strand origin; AGE, agarose gel electrophoresis; RITOLS, RNA incorporated throughout the lagging strand; TEM, transmission electron microscopy; NCR, non-coding region; mtRI, mtDNA replication intermediate; TFAM, mitochondrial transcription factor A; HEK, human embryonic kidney.

phages such as T4 (29). In addition, molecular recombination is a widespread, if not universal, mechanism of DNA repair notably of double strand breaks and involving exchange of material between homologous segments of damaged and undamaged DNA (30–32). Failures in this system in nuclear DNA are the cause of a diverse spectrum of human diseases (33).

Plants, fungi, and some other organisms have been shown to have active mtDNA recombination (for a review, see Ref. 34), and genetic recombination has been reported in cultured mammalian cells harboring different mtDNA deletions or point mutations (35, 36). Intramolecular recombination has also been detected in mammalian cells containing partially duplicated mtDNAs (37, 38). In the plant kingdom, a mitochondrial homologue of the RecA protein has been found in both *Arabidopsis* (39) and *Physcomitrella* (40). Recombination activity has been detected in lysates of mammalian mitochondria (41), and abundant branched molecules having the characteristics of a Holliday (four-way, X-) junction have been observed in human cardiac muscle mtDNA by two-dimensional AGE (42). Molecular structures resembling four-way junctions have also been inferred in the vicinity of O_H in mtDNA from cultured mammalian cells and have been interpreted as pretermination intermediates (15, 43).

In the present work we addressed further the nature and significance of the junctional molecules in human heart mtDNA using a combination of one- and two-dimensional AGE, transmission electron microscopy (TEM), and enzymatic treatments. The results indicate that human heart as well as, to a lesser extent, human and mouse brain, maintain mtDNA in multigenomic complexes linked by intercatenation plus four-way and three-way junctions. Standard θ-type replication intermediates were not detectable in human heart mtDNA, indicating that mtDNA replication proceeds via a non-θ mechanism in this tissue. Lastly the pattern of mtDNA replication intermediates detected in the tissue of mice transgenic for either of two proteins involved in mtDNA maintenance, mitochondrial transcription factor A (TFAM) and Twinkle, shows a substantial increase in junctional forms.

EXPERIMENTAL PROCEDURES

DNA Extraction and Autopsy Series—Total DNA from cultured cells was extracted by standard methods (43) and from frozen forensic autopsy samples as described in Hyvärinen *et al.* (44). For full details see the supplemental data. The samples were taken as part of the Tampere Coronary Study, approved by the Ethics Committee of Tampere University Hospital (DNO 1239/32/200/01) and the National Authority for Medico-legal Affairs, and included cardiac muscle samples from 12 individuals of different ages (for full details see Table 1). None had any known history of heart disease. Pig and rabbit heart DNAs were extracted similarly.

mtDNA Extraction—mtDNA was isolated from cultured cells as described by Yasukawa *et al.* (19) and from human and mouse tissues essentially as described by Reyes *et al.* (18) and Yasukawa *et al.* (19): for full details see the supplemental data. Tissue samples were from mice transgenic for Twinkle (Ref. 45, line A) and TFAM (44) as well as non-transgenic littermate controls.

TABLE 1
Details of human heart DNA samples used for analysis
F, female; M, male.

Sex	Age	Cause of death	Type of analysis
	yr		
F	2	Foreign object in larynx	Two-dimensional AGE of total DNA
M	19	Crush injury to skull	Two-dimensional AGE of total DNA
F	22	Fatal wound	Two-dimensional AGE of total DNA
M	23	Suicide by shotgun	Two-dimensional AGE of total DNA
M	26	Car accident (suicide)	TEM and two-dimensional AGE of mtDNA
F	31	Drowning	Two-dimensional AGE of total DNA
M	33	Drowning	Two-dimensional AGE of total DNA
M	44	Hypothermia	Two-dimensional AGE of total DNA
M	52	Car accident	Two-dimensional AGE of total DNA
M	53	Suicide by handgun	Two-dimensional AGE of total DNA
M	58	Gunshot wound to head (homicide)	TEM and two-dimensional AGE of mtDNA
F	69	Pneumonia	TEM and two-dimensional AGE of mtDNA

Two-dimensional AGE—1 μg of total mitochondrial nucleic acids or 10 μg (heart and brain) or 20 μg (skeletal muscle, kidney, and cultured cells) of total DNA was used per analysis. Restriction digestions and other enzyme treatments were performed following the manufacturers' recommendations (see Ref. 43 for enzyme details and suppliers). If subsequent treatment with another nuclease was used, DNA was first recovered by ethanol precipitation and resuspended in the appropriate reaction buffer before treatment with the second enzyme. Reactions were stopped by the addition of an equal volume of phenol-chloroform-isoamyl alcohol (25:24:1, pH 8.0) and immediately extracted. Two-dimensional AGE and Southern blotting were performed as described previously (Ref. 43: note the different gel conditions for different fragment sizes).

One-dimensional AGE—1–5 μg of total DNA or 100 ng of mtDNA were used in the analysis. Subsequent treatments with topoisomerase IV (John Innes Enterprises), topoisomerase I, T7 endonuclease I, or λ-exonuclease (all New England Biolabs) used the manufacturers' recommended conditions. When multiple enzyme treatments were used, DNA was ethanol-precipitated between the steps. The gel conditions and blotting were as described in Pohjoismäki *et al.* (43).

Radiolabeled Probes and Blot Hybridization—For Southern hybridization, probes were created by *Pfu* PCR using as template cloned segments of human mtDNA (see Refs. 19, 44, and 45) or 18 S rDNA (primers, CTACTTGGAAAACTGTGGTAATTCTA and TTTTAACTGCAGCAACTTTAATATAC, both 5′ to 3′; *i.e.* nucleotides 24–772 of the human 18 S rDNA sequence, NCBI accession number M10098). Mouse mtDNA probes created from mouse mtDNA by *Pfu* PCR followed by gel purification spanned nucleotides 15357–136 (non-coding region (NCR)) and 5383–5910 (COXI). Pig and rabbit probes were created similarly from total DNA and correspond to the mtDNA fragments ND1 (nucleotides 2821–3422) and COXI (nucleotides 2551–2980), respectively. Probes were labeled using a Rediprime™ II random prime labeling kit (Amersham Biosciences) and [α-^{32}P]dCTP (Amersham Biosciences; 3000 Ci/mmol).

Transmission Electron Microscopy—Approximately 1 μg of nucleic acids extracted from sucrose density gradient-purified

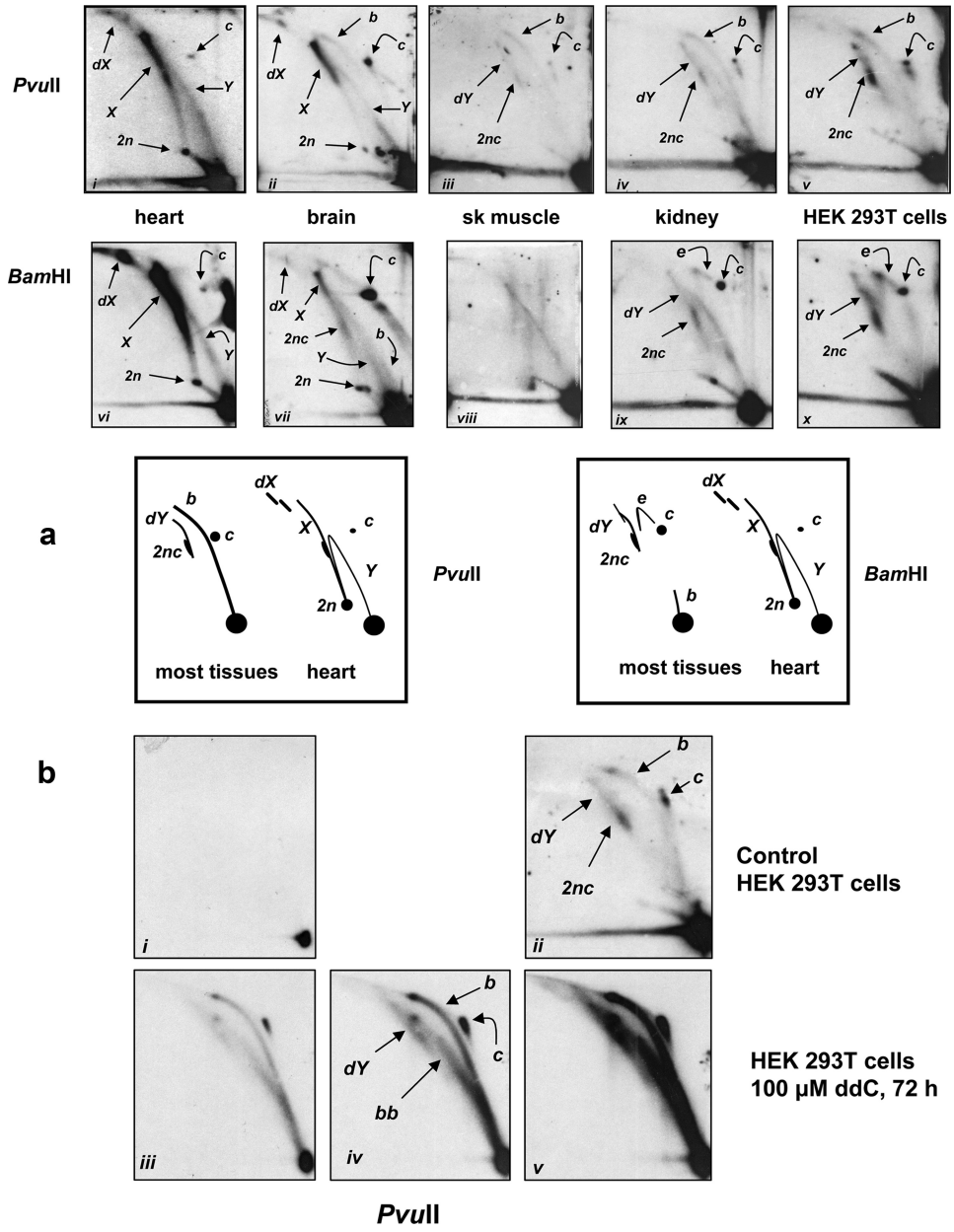

FIGURE 1. **Two-dimensional AGE analysis of mtRIs from human tissues and cultured cells as indicated, treated with restriction enzymes cutting once in the mitochondrial genome.** *a*, mtDNA was linearized with PvuII or BamHI as shown and hybridized with combined ND4 and O_H region probes. The various arcs, interpreted in the panels below, represent dimeric linear molecules (*2n*), monomeric (*c*) and dimeric circles (*2nc*), Y intermediates (*Y*), double Y intermediates (*dY*), replication bubbles (*b*), *i.e.* standard initiation arc, X forms (*X*; *i.e.* dimeric fragments joined by four-way junctions), complex forms proposed to consist of multimeric fragments joined by multiple four-way junctions (*dX*), and θ molecules with broken arms attached to an intact circle (*e*; forming an eyebrow arc). For fuller explanation of the gels, see supplemental Fig. 1. Note that only bubble and double Y arcs can be considered as products of standard θ replication in such analyses, although RITOLS-type θ replication can also generate eyebrow arcs (Yasukawa *et al.* (20)). *b*, two-dimensional AGE of PvuII-digested mtDNA extracted from HEK 293T cells with or without 72 h of treatment with 100 μM ddC to induce widespread and prolonged replication stalling. Steady-state replication intermediates were greatly increased (*panels i* and *iii* are similar exposures as are *panels ii* and *v*), but the predominant forms were still θ bubbles and double Y forms with only a minority of molecules suffering fork regression or nicking to generate broken bubbles (*bb*). *sk*, skeletal.

human heart mitochondria was treated with 50 units of RNase If (New England Biolabs) at 37 °C for 30 min in the manufacturer's buffer, recovered by phenol-chloroform extraction and ethanol precipitation, and redissolved in TEM grade TE buffer (10 mM Tris-HCl, 0.1 mM ETDA, pH 7.6). A separate aliquot was digested further with BamHI or PvuII and recovered similarly. Aliquots (0.5–1.0 ng) of mtDNA were prepared and directly mounted on parlodion-coated grids following the Kleinschmidt procedure (46, 47). Imaging and image analysis were performed as described previously (48).

RESULTS

mtDNA Replication Intermediates Differ between Tissues—We set out initially to characterize the forms of mtDNA and its replication intermediates present in different human tissues. We digested postmortem DNA samples from human heart and other tissues as well as cultured (HEK 293T) cells with each of two restriction enzymes cutting only once in the mitochondrial genome but in different regions, namely PvuII and BamHI (Fig. 1*a*). Upon two-dimensional AGE, θ replication intermediates, forming bubble and double Y arcs plus the eyebrow arc associated with RITOLS-type replication (see supplemental Fig. 1), were readily detected in mtDNA of cultured cells, brain, and kidney but were very faint in skeletal muscle. A standard initiation (bubble) arc was seen in the PvuII digest (Fig. 1*a*, *panels ii–v*). In the BamHI digest (Fig. 1*a*, *panels vii–x*), a double Y arc was prominent as well as either a short bubble arc (in brain) or an "eyebrow" arc resulting from non-digestion at the restriction site (see supplemental Fig. 1 for a fuller explanation).

Standard θ replication intermediates were not detectable in human cardiac muscle mtDNA (Fig. 1*a*, *panels i* and *vi*). The major mtDNA replication intermediates (mtRIs) were Y-form molecules encompassing the whole genome; the products of the two digests were virtually indistinguishable electrophoretically. A prominent (X) arc of putative recombination intermediates (*i.e.* molecules containing four-way junctions) was also seen as well as linear molecules migrating at 2n[3] and complex forms

[3] 1n in the context used here means the unit length of the mitochondrial genome, 16,569 base pairs of DNA. 2n thus means twice that, *i.e.* a molecule of 33 kbp.

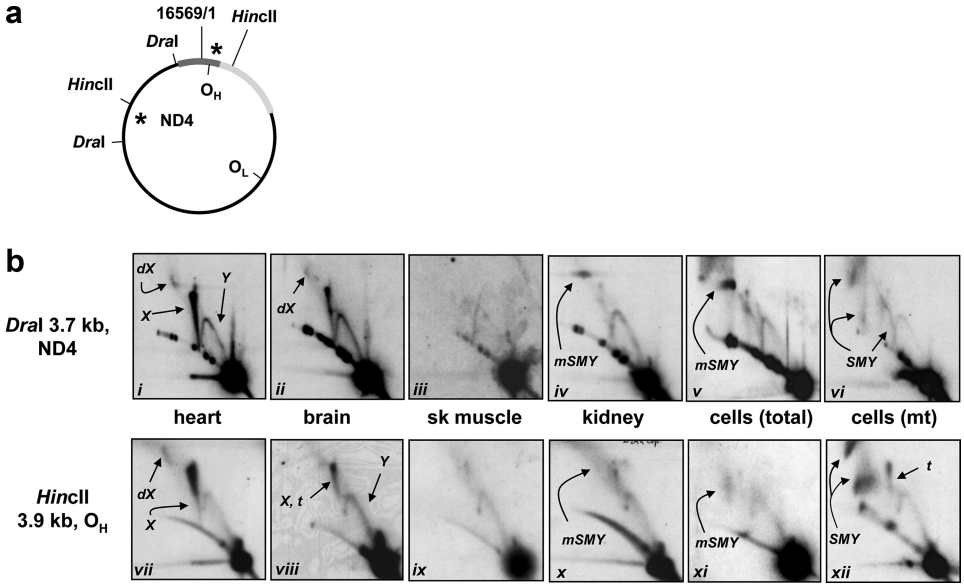

FIGURE 2. **Two-dimensional AGE analysis of mtRIs in different human tissues and cultured HEK 293T cells, as indicated, using restriction enzymes cutting at multiple sites in the mitochondrial genome.** *a*, schematic map of human mtDNA showing the locations of relevant restriction sites and probes (*asterisks*). The major NCR is shown as a *dark gray bar*, and rDNA is shown as a *light gray bar*. *b*, two-dimensional AGE blots, digests, and probes as shown. All DNA samples were total DNA except *panels vi* and *xii*, which used mtDNA extracted from sucrose gradient-purified mitochondria. The various arcs indicated (for clarity, and where obvious, not shown in every panel) represent X forms (*X*), Y intermediates (*Y*), putative double X forms (*dX*), "slow moving" Y arcs (*SMY*) created by non-digestion at restriction sites blocked by RNA or single strandedness, modified SMY arcs (*mSMY*) resulting from RNase H degradation, and termination intermediates (*t*) in which two oppositely moving forks are juxtaposed. For a fuller explanation of the gels, see supplemental Fig. 1. Bubble arcs, although not seen clearly at this exposure, were present in long exposures of *panels iii–vi* and *ix–xii* (*e.g.* see supplemental Fig. 3e). *sk*, skeletal.

migrating at >2n in the first dimension that may represent multimeric molecules held together by more than one four-way junction (denoted as *dX* in Fig. 1*a*).

To investigate whether the absence of the initiation arc in heart could be explained as a trivial artifact arising from loss of bubble structures during extraction, *i.e.* due to single strand breakage at replication forks, we treated heart and HEK 293T cell PvuII digests with single strand-specific nuclease S1 (supplemental Fig. 2). The HEK 293T cell bubble arc was indeed partially converted to a Y-like (broken bubble) arc, although its trajectory was slightly different from that of the standard Y arc seen in the heart sample, and the largest bubbles were relatively resistant. Importantly S1 nuclease also preferentially degraded the X arc and the 2n linear molecules in the heart sample. These observations indicate that the absence of standard θ intermediates in heart mtDNA is not a degradation artifact. The mtRIs revealed in human brain (Fig. 1*a*, *panels ii* and *vii*) resembled a mixture of those from heart and from other tissues or cultured cells.

In previous experiments we found that, in material prepared from crude mitochondria, mtRIs were relatively degraded compared with material extracted from sucrose gradient-purified mitochondria; this was largely attributable to RNase H activity (15). Because of the paucity of material and ethical considerations, the human autopsy samples were generally prepared as total DNA. We therefore conducted one experiment using DNA extracted from sucrose density gradient-purified mitochondria of human cardiac muscle and cerebral cortex isolated as soon as possible after death (6 h). Two-dimensional AGE analysis of this material following PvuII digestion (supplemental Fig. 3a) gave essentially indistinguishable results from those seen with total DNA except that the brain sample was less degraded with both bubble and especially X forms better preserved.

Two-dimensional AGE of subgenomic restriction fragments of mtDNA confirmed consistent tissue differences in the patterns of mtRIs seen in heart compared with other tissues or with cultured cells (Fig. 2). We analyzed two overlapping fragments of the genome, namely the HincII fragment spanning the major NCR and containing O_H plus the overlapping DraI fragment that excludes the NCR. The mtRIs from sucrose density gradient-purified mitochondria of cultured HEK 293T cells (Fig. 2*b*, *panels vi* and *xii*) included the prominent RNA-containing RITOLS intermediates as detected previously, giving rise to slow moving Y-like arcs (denoted *SMY*). In total DNA prepared from the same cells (Fig. 2*b*, *panels v* and *xi*) these intermediates were, as previously (16), subject to partial degradation during extraction because of RNase H activity, giving rise to modified slow moving Y-like arcs (*mSMY*). The latter were also seen in total DNA from kidney (Fig. 2*b*, *panels iv* and *x*) and very faintly in total DNA from skeletal muscle (Fig. 2*b*, *panels iii* and *ix*) where all mtRIs were at low abundance. However, they were not detected in total DNA from heart (Fig. 2*b*, *panels i* and *vii*) or brain (Fig. 2*b*, *panels ii* and *viii*).

In both heart and brain samples standard Y and prominent X arcs were seen in the DraI digest as well as high molecular weight structures. In the HincII digest, initiation arcs were not seen in the samples from heart or brain even on long exposure (supplemental Fig. 3e), although initiation arcs (modified by ribonucleotide loss) were visible at long exposure in total DNA from cultured cells; supplemental Fig. 3d). However, the Y arc was incomplete, suggesting that O_H is still acting, even in heart, as an obligatory terminus of replication. The abundant X arcs seen in human cardiac muscle were not seen in equivalent digests of total DNA from similarly processed cardiac muscle of other mammals (mouse, rabbit, and pig), whereas conventional θ replication intermediates of the RITOLS type were clearly seen in these samples (supplemental Fig. 3b). Note that rabbit and pig hearts were processed at least 24 h after death yet X arcs were absent, indicating that they did not arise in the human samples as a result of a post-mortem artifact under hypoxic conditions In humans, X arcs were seen in cardiac muscle DNA from each of 15 different individuals irrespective of age (*e.g.* supplemental Fig. 3c). Prominent X arcs were absent from all

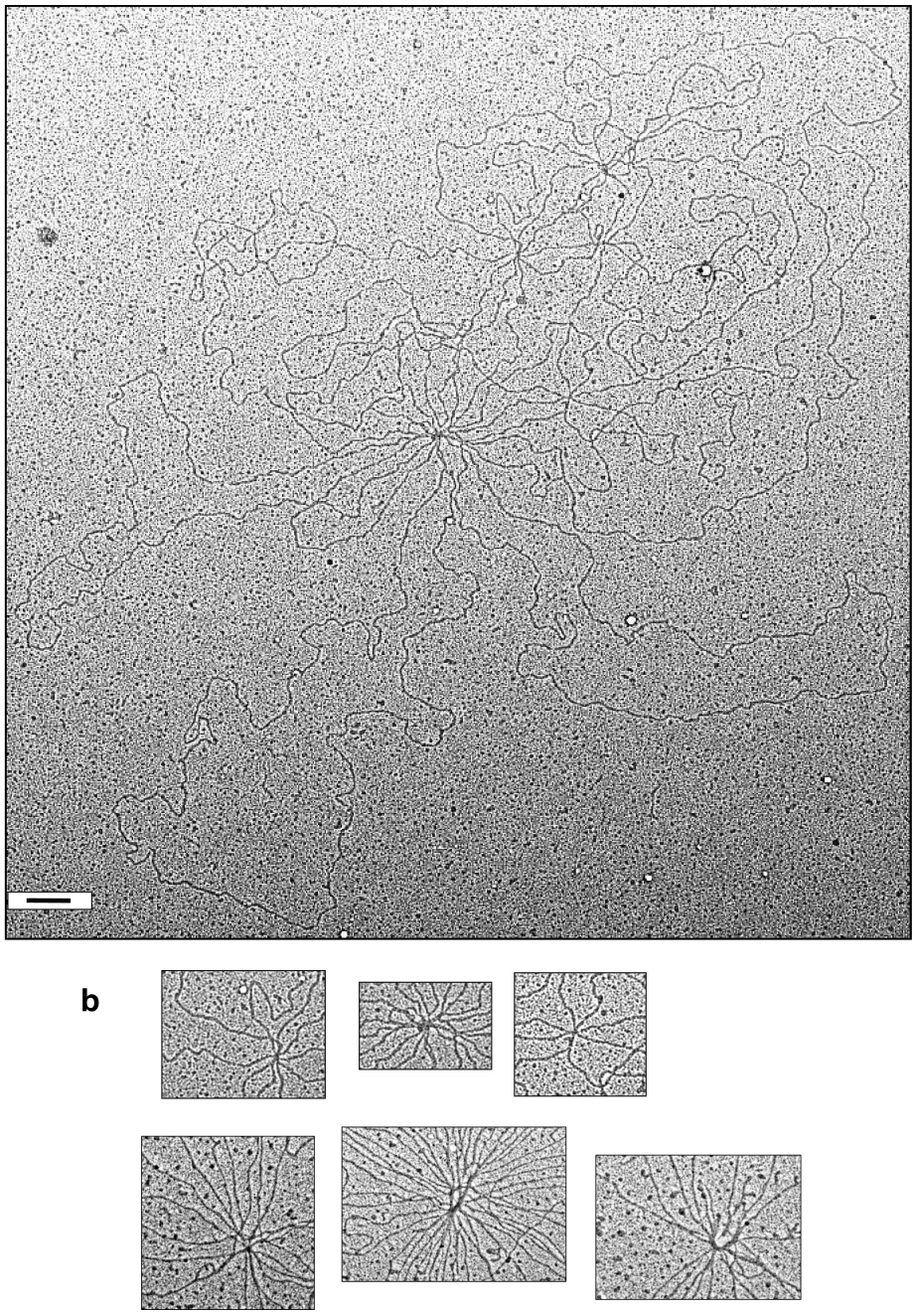

FIGURE 3. **TEM of human heart mtDNA.** *Scale bars*, 200 nm. *a*, tangled complex of monomeric and dimeric circles containing ~20 genome equivalents. Some other tangled networks appeared even more complex. *b*, nexuses of five different tangles at higher magnification. *c*, *panel i*, three monomeric circles held together by junctions (*arrows*) (catenation, hemicatenation, and/or four-way recombination junctions). *Panels ii–viii*, examples of such junctions at higher magnification. *Panels ii* and *iii* are from the same complex as shown in *panel i*. *Panels iv–vi* are from other paired circular molecules. *Panels vii* and *viii* are similar junctions seen in the multimeric tangles. *d*, Southern blot of purified mtDNA (1 μg of nucleic acid) alongside total DNA (20 μg) undigested (*U*) or digested with PvuII (*P*) or EcoRI (*E*; E2 is an independent mtDNA sample from a second individual) and either stained with ethidium bromide (*EtBr*) or blot-hybridized with probes for 18 S rDNA (*18S*) or cytochrome *b* (*cyt b*; Ref. 19).

digests and fragments of human cultured cell, kidney, and skeletal muscle mtDNA.

To exclude the possibility that the X arcs seen in human heart might arise as an artifact of preparation due to the regression of stalled replication forks, we treated cultured cells for 72 h with dideoxycytidine to induce systematic chain termination and fork arrest in replicating mtDNA. As expected, this treatment resulted in a large increase in the steady-state level of mtRIs (Fig. 1*b*). However, θ forms were well preserved, and species migrating on two-dimensional gels as X-junctional molecules such as those seen in myocardial mtDNA preparations did not arise (Fig. 1*b*).

Human Heart mtDNA Is Organized in Multimeric Junctional Complexes—The absence of standard θ replication mtRIs in human cardiac muscle prompted us to look at the overall organization of mtDNA in this tissue. We used TEM to analyze human cardiac muscle mtDNA prepared from sucrose density gradient-purified mitochondria (Fig. 3, *a–c*). The absence of nuclear DNA contamination was confirmed by Southern blotting to an 18 S rDNA probe (Fig. 3*d*). In contrast to mtDNA in cultured HEK 293T cells, where the majority of molecules were monomeric circles, most heart mtDNA was organized in multimeric complexes (Table 2 and Fig. 3). Some of these, containing a substantial fraction of the total mtDNA mass, were complex tangles (*e.g.* Fig. 3*a*) containing one or several nexuses and frequently more than 20 genome equivalents. At higher magnification (*e.g.* Fig. 3*b*) the nexuses did not appear to contain electron-dense fibrous material, such as that seen in preparations of chromatin loops associated with fragments of nuclear matrix. They persisted after digestion with proteinase K and further phenol extraction. However, the tangles were impossible to parse. The simplest multimeric arrays, containing just two to three copies of the genome, appeared to be held together by junctions (Fig. 3*c*), although their exact nature cannot be inferred from TEM alone. Tailed monomeric (or dimeric) circles were not seen, providing further evidence that the Y arcs seen on two-dimensional gels were not created by breakage of θ bubbles. Conversely three-way junctions that could give rise to the Y arcs seen on two-dimensional gels were visible in the complex tangles mostly at or near nexuses (Fig. 3*b*). The complex tangles were seen in different spreads of the same mtDNA preparation and in mtDNA preparations from three different individuals although not in HEK

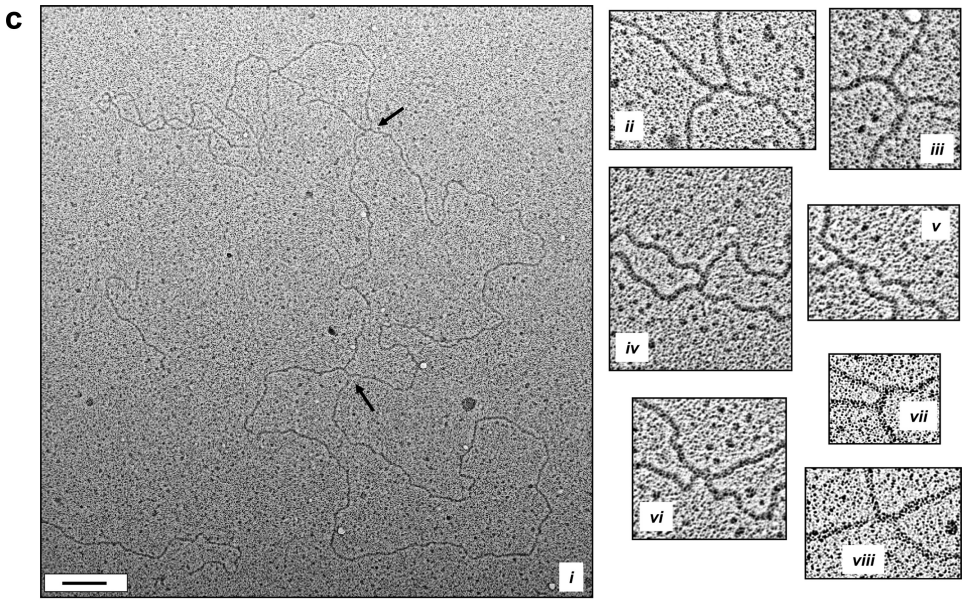

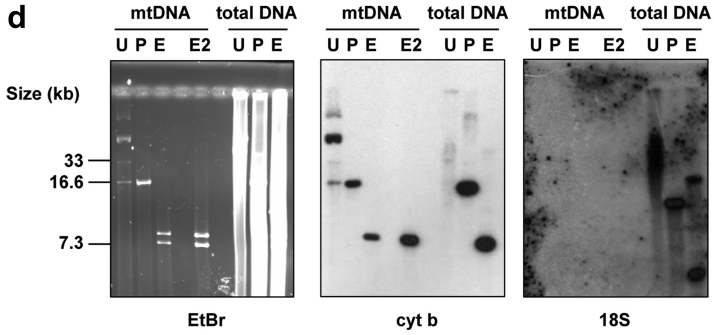

FIGURE 3—*continued*

We studied the topology of human heart mtDNA further using a combination of one- and two-dimensional AGE combined with various enzymatic treatments. The most complex tangles could not be resolved electrophoretically (Fig. 4). Material unable to enter the first dimension gel was completely lost when one-dimensional gels were processed for blotting (Fig. 4*a*) but was retained in two-dimensional gels (material denoted *tgl* in Fig. 4*b*). Most of the material that did enter one-dimensional gels migrated as two broad bands (Fig. 4*a*) denoted t and f. Only a small proportion of the material migrated as monomeric supercoils, in contrast to mtDNA from cultured HEK 293T cells electrophoresed under identical conditions (41). This accords with the findings from TEM. A small amount of monomeric (1n) and dimeric (2n) linear mtDNA was detected (Fig. 4, *a* and *b*, *panel i*).

The tangles were efficiently converted to simpler, electrophoretically interpretable forms by combined treatment with topoisomerase IV, a decatenating enzyme that also removes supercoils, and phage T7 endonuclease I, which cuts cruciform junctions. Neither enzyme alone resolved the tangles, although treatment with T7 endonuclease I alone did allow some of the high molecular weight material to enter the first dimension gel. The tangles are therefore inferred to be held together by a combination of catenation and four-way junctions. The limit products from combined treatment with the two resolving enzymes were monomeric and dimeric circles and linear molecules as well as a large quantity of heterogeneous linear DNA ranging in size from 2n to <1n. Trimeric or higher order linear molecules (or circles) were absent and were not generated by any enzymatic treatment.

Two-dimensional AGE and enzymatic digestion revealed that bands t and f were each composed of several different species. The more retarded portion of band t was modified by topoisomerase IV but not by topoisomerase I or by T7 endonuclease I, indicating that it consisted of catenated dimers or multimers. One novel species was generated by topoisomerase IV treatment (denoted *x* in Fig. 4*b*, *panel ii*) that migrated in the same part of the first dimension gel (band f) as monomeric circles and dimeric linear molecules but was more retarded than either of the latter forms in the second dimension. This species as well as being released by decatenation was sensitive to both T7 endonuclease I and λ-exonuclease (Fig. 4*a*), identifying it as a circle joined to a linear molecule by a four-way junction. The remaining material of band t was resistant to all of

TABLE 2

Representation of different molecular forms in mtDNA from human heart and cultured HEK 293T cells analyzed by electron microscopy

RI, replication intermediate.

mtDNA source	*n*[a]	1n circles	2n circles	Pairs[b]	Complexes[c]	RIs
HEK 293T cells	1005	853	2	73	22	52
Heart	500	178	167	88	61[d]	6[e]

[a] Total number of molecular species assigned.

[b] Two circular molecules linked by tight catenation or recombination junctions (*e.g.* Fig. 3*c*). This class excludes molecules that appeared as two overlapping circles in the spread (which were excluded completely from the analysis because such figures are ambiguous).

[c] Aggregates of three or more molecules linked by tight catenation or recombination junctions. In general, such complexes visualized in HEK 293T cell mtDNA comprised just three to five molecules (*e.g.* supplemental Fig. 4), whereas those in heart frequently contained >20 molecules in highly tangled complexes (Fig. 3, *a* and *b*).

[d] Because most of these complexes contained >20 molecules they represented a substantial fraction of the total mass of mtDNA in heart, perhaps 50% or more.

[e] No θ intermediates were seen in heart. The six molecules scored as "replication intermediates" were all aberrant structures, such as those illustrated in supplemental Fig. 4b, containing junctions and linear ends and of less than one genome length equivalent in total. They may be assumed to have broken off from the tangled complexes.

293T cell mtDNA spread in parallel, making it highly unlikely that they were created as an artifact of incomplete spreading. They remained uncut by BglII, which has no recognition site in human mtDNA but which cuts frequently in nuclear DNA. Cerebral cortex mtDNA (not shown) was a mixture of the forms seen in heart and in cultured cells, consistent with findings from two-dimensional AGE.

the enzymatic treatments tested and migrated as dimeric open circles, a species also seen abundantly by TEM (Table 2). The above findings indicate that most mtDNA in human heart is organized in junctional complexes held together by catenation and four-way junctions.

The effects of topoisomerase IV were verified by TEM (Fig. 4, *c* and *d*). The complex tangles were greatly simplified, releasing a combination of decatenated monomeric and dimeric circles as well as persisting junctional forms. These included many examples of circular molecules still joined together by what are most simply interpreted as four-way junctions (Fig. 4*c*) as well as other molecules containing three-way junctions, linear ends, and/or linear segments apparently joining circles to linear molecules (*e.g.* Fig. 4*d*) or to other circles.

To investigate the relationship between these junctional forms and mtDNA replication, we digested heart mtDNA with PvuII or BamHI prior to spreading for TEM (Fig. 5). In addition to simple linear molecules, we saw many molecules still linked by junctions. Some material remained in loosely tangled networks, which could not be parsed reliably. Interpretable junctions were of three types: four-way junctions usually with at least two branches of equal length (Fig. 5, *a–d*), three-way junctions with branches of equal (Fig. 5*e*) or unequal length (Fig. 5*f*), and complex junctions (Fig. 5, *g–i*). Many four-way junctions appeared to comprise two closely spaced junctions joined by a short bridge of intertwined duplex or partially resected material equivalent to the classic double Holliday junction intermediate of the double strand break repair model of homologous recombination (49). Complex (multiple) junctions were found at the nexuses of persistent tangles as well as in simpler molecules (Fig. 5, *g–i*). Apart from a few classic Y-form molecules (*e.g.* Fig. 5*e*), which could arise by a variety of mechanisms, the non-linear mtDNA species

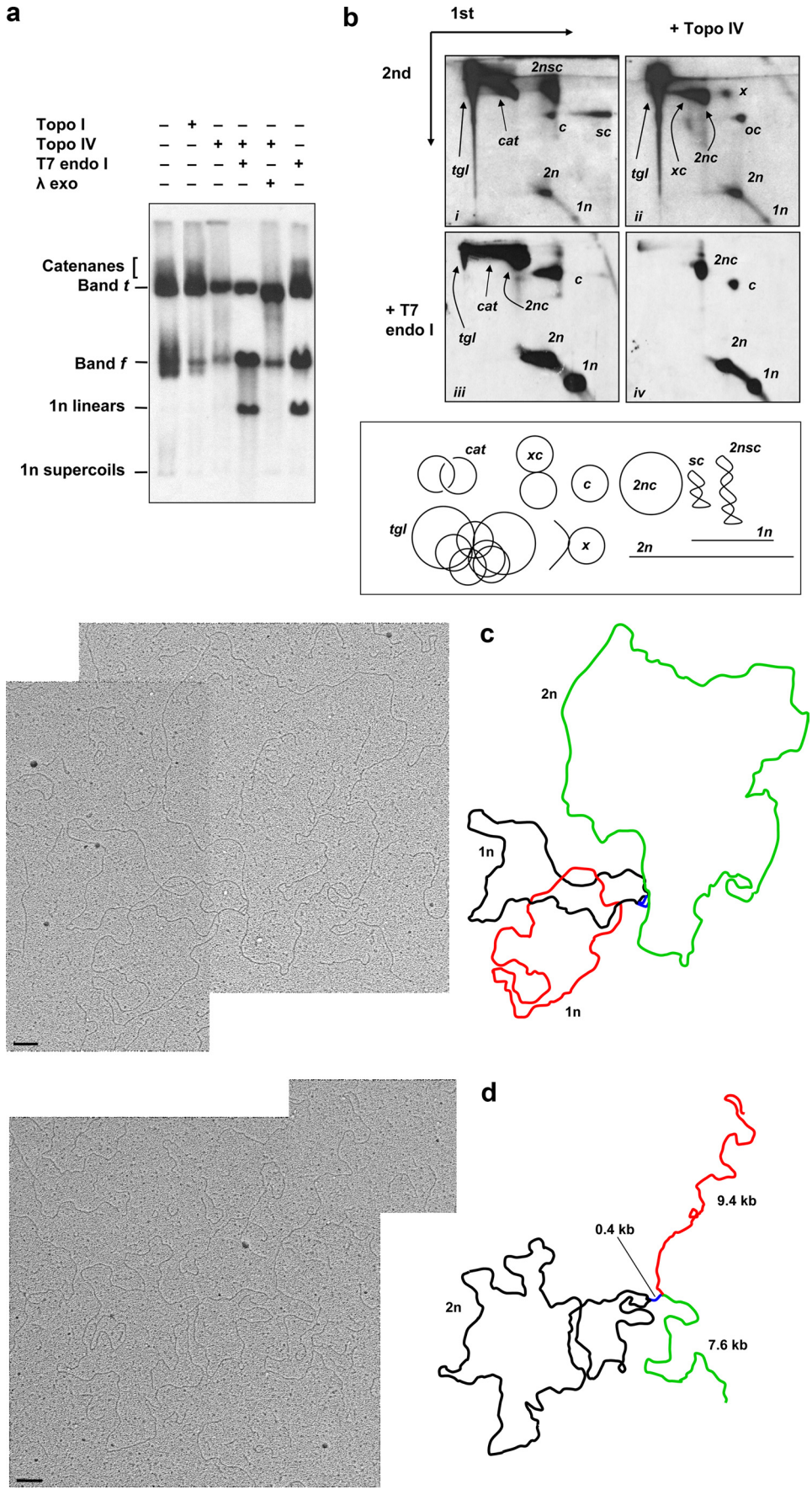

observed after digestion were inconsistent with standard θ replication, and molecular species predicted to arise from θ intermediates were absent. Conversely the junctional forms seen in heart were not seen in material from cultured cells processed identically.

Junctional mtDNA Molecules Are Enhanced in Tissues of TFAM and Twinkle Transgenic Mice—We noted that the tissues in which junctional mtDNA species were prominent were also those exhibiting highest mtDNA copy number (supplemental Table 1). To investigate further the relationship between mtDNA copy and organization, we analyzed mtDNA in two transgenic mouse models in which overexpression of proteins involved in mtDNA metabolism results in a copy number increase, *i.e.* the mitochondrial DNA helicase Twinkle (43) and human TFAM (44, 48).

We used two-dimensional AGE to compare mtRIs in different tissues of TFAM and Twinkle transgenic mice of different ages and in non-transgenic littermates (Fig. 6). mtRIs were detectable only at relatively low levels in control heart (Fig. 6, *b* and *c*, *panels i*; *d*, *panel ii*; and *e*, *panel iii*) but were consistently enhanced and altered by Twinkle overexpression (Fig. 6, *b* and *c*, *panels ii*; *d*, *panel iii*; and *e*, *panel iv*) regardless of age, whereas those in liver were indistinguishable from control mice (Fig. 6, *b* and *c*, *panels iv* and *v*; and *e*, *panels i* and *ii*). The changes in heart represented a shift toward forms resembling those seen in human heart, *i.e.* the appearance of X arcs (putative recombination intermediates containing four-way junctions) in all regions of the genome tested. Initiation (bubble) arcs, indicative of standard θ replication, persisted as did the arcs attributable to RITOLS intermediates. TFAM overexpression produced a similar but more dramatic effect in heart (Fig. 6, *b* and *c*, *panels iii*) with the appearance of prominent X arcs accompanied by relative loss of initiation arcs and of RITOLS intermediates plus a slight induction of X arcs in liver (*panels vi*). In brain, X arcs were present alongside standard θ replication intermediates even in control mice, but Twinkle overexpression resulted in a large increase thereof (Fig. 6, *e*, *panels i* and *ii*; and *f*, *panels v* and *vi*). Twinkle overexpression also produced a small increase in X-junctional forms in skeletal muscle, whereas they were only visible in control mouse muscle at long exposure (supplemental Fig. 4, panels iii and iv).

One-dimensional agarose gel electrophoresis (Fig. 7) also confirmed the appearance of complex junctional forms in Twinkle- (Fig. 7, *a* and *b*) or TFAM-overexpressing (Fig. 7*c*) heart but not liver. Like those in human heart (Fig. 4), these were resolved by topoisomerase IV and T7 endonuclease I (Fig. 7*b*).

DISCUSSION

This study combines two major, primary findings on human heart mtDNA: the absence of standard θ replication intermediates and its organization in junctional complexes that have some similarities with mtDNA networks reported previously in plants (8). The fact that these observations were made in the same tissue raises the issue of whether and how they are related. In both cases we have excluded the obvious artifactual explanations (nuclear DNA contamination, freeze-thaw or post-mortem damage, branch migration, or fork regression during extraction). Note that the unusual forms were absent from samples of mouse, pig, or rabbit heart processed in a similar manner.

The absence of standard θ replication intermediates combined with the abundant presence of molecules containing three-way, four-way, and more complex junctions implies strongly that human heart mtDNA must replicate by a non-θ mechanism. θ intermediates were not released by resolving enzymes (restriction or junctional endonucleases or topoisomerases). Nor did we observe any credible examples of replication bubbles inside the junctional complexes. However, the unresolved networks are so complex that we cannot exclude the possibility that junctions are systematically branch-migrated and resolved as replication forks advance. Nevertheless this would clearly not be standard θ replication.

The Relationship between mtDNA Organization and Replication in Human Heart—Analysis of junctional complexes by resolving enzymes, electrophoresis, and TEM does not allow us to extrapolate a specific alternative replication model at this time. All we can infer is that the intermediates predicted by any previously proposed mtDNA replication model are absent, implying that a novel type of replication is occurring. Note that although standard θ forms were absent so were the structures predicted by the strand asynchronous replication model (14): human heart mtDNA forms containing four-way junctions are largely resistant to S1 nuclease (Ref. 42; see also supplemental Fig. 1). We also cannot completely exclude that the unusual structures seen are, at least in part, a manifestation of mtDNA repair processes. However, this would not explain the absence of standard replication intermediates. Conversely the presence of four-way junctions does not imply that recombination, as classically understood, is taking place because these structures could equally well be generated during DNA replication. The forms detected are not those of conventional rolling circle or recombination-dependent replication as seen, respectively, in yeast mtDNA (4, 50) or in bacteriophage T4 (29), chloroplast

FIGURE 4. **Electrophoretic and TEM analysis of human heart mtDNA.** *a*, one-dimensional AGE of undigested cardiac muscle mtDNA treated with the enzymes as indicated (topoisomerase (*Topo*) I, topoisomerase IV, T7 endonuclease (*endo*) I, and λ-exonuclease (*exo*)). The identity of the various species is inferred by the effects of enzymatic treatments on their relative amounts and by their migration properties on two-dimensional AGE (*b*). Bands *t* and *f* are each composites of several species. λ-Exonuclease digests molecules with exposed 5′ phosphorylated ends. Because it removes or modifies the residual material running just behind open circles after topoisomerase IV treatment, *i.e.* 2n linear molecules plus species *x* (*b*, *panel ii*), we infer that species *x* has exposed ends. *b*, two-dimensional AGE of cardiac muscle mtDNA untreated (*panel i*), treated with topoisomerase IV (*panel ii*), treated with T7 endonuclease I (*panel iii*), and treated with topoisomerase IV + T7 endonuclease I (*panel iv*). The topology of the various forms, annotated on the gel images and inferred from the treatments and electrophoretic mobilities, is shown *below* the gel panels. *tgl*, tangled complexes (see Fig. 3); *cat*, catenanes (can also include >2 monomeric or dimeric circles); *1n* and *2n*, monomeric and dimeric linear molecules, respectively; *c* and *2nc*, monomeric and dimeric open circles, respectively; *sc* and *2nsc*, supercoiled monomeric and dimeric circles, respectively. *xc*, circular molecules joined by four-way junctions; *x*, suggested to be circles joined to linear molecules by four-way junctions. *Arrows* indicate directions of first and second dimension electrophoresis. *c* and *d*, examples of forms seen by TEM following topoisomerase IV treatment of heart mtDNA alongside interpretations. Distinct circles and linear segments are indicated in different colors with inferred contour lengths in kb or (for circles) genome lengths. *Scale bars*, 200 nm.

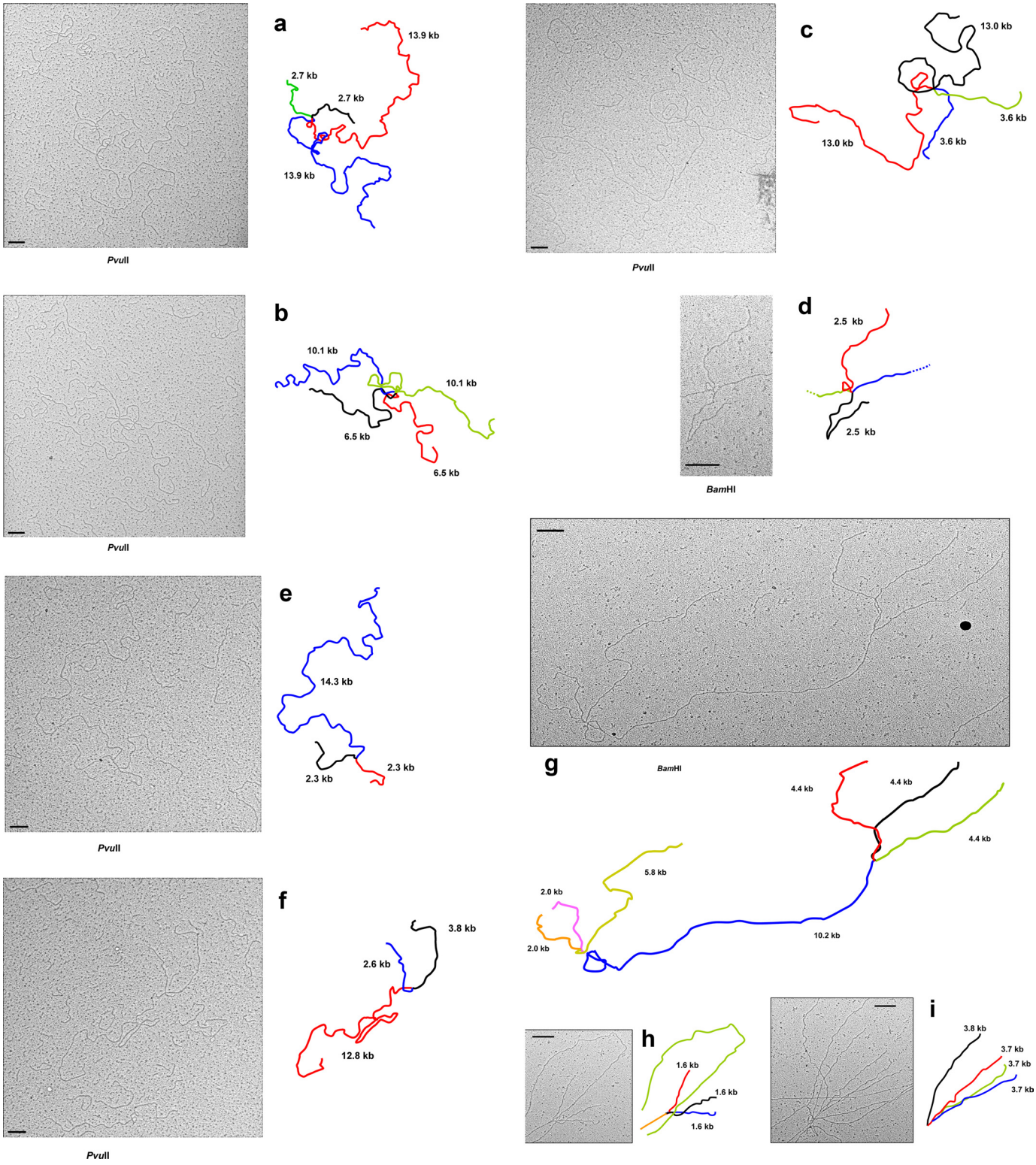

FIGURE 5. **TEM of PvuII- and BamHI-digested human cardiac muscle mtDNA.** *a–i*, images of various junctional molecules alongside interpretations are shown. In each case except *f* at least two branches (plus two other branches if entirely within the field) are of equal length. Note that many junctions appear to be composite, *i.e.* to consist of two adjacent four-way (and/or three-way) junctions. Distinct linear segments emanating from junctions are indicated in different colors with inferred contour lengths in kb. *Scale bars*, 200 nm.

(51), and some plant mitochondrial DNAs (52–55). However, replication forks (three-way junctions) were clearly present within the junctional complexes and persisted in the residual material after treatment with restriction or resolving enzymes. This indicates that DNA replication actually takes place within the junctional networks, thus giving it features of both rolling circle and recombination-dependent replication with the T4 phage system probably the closest precedent. The absence of

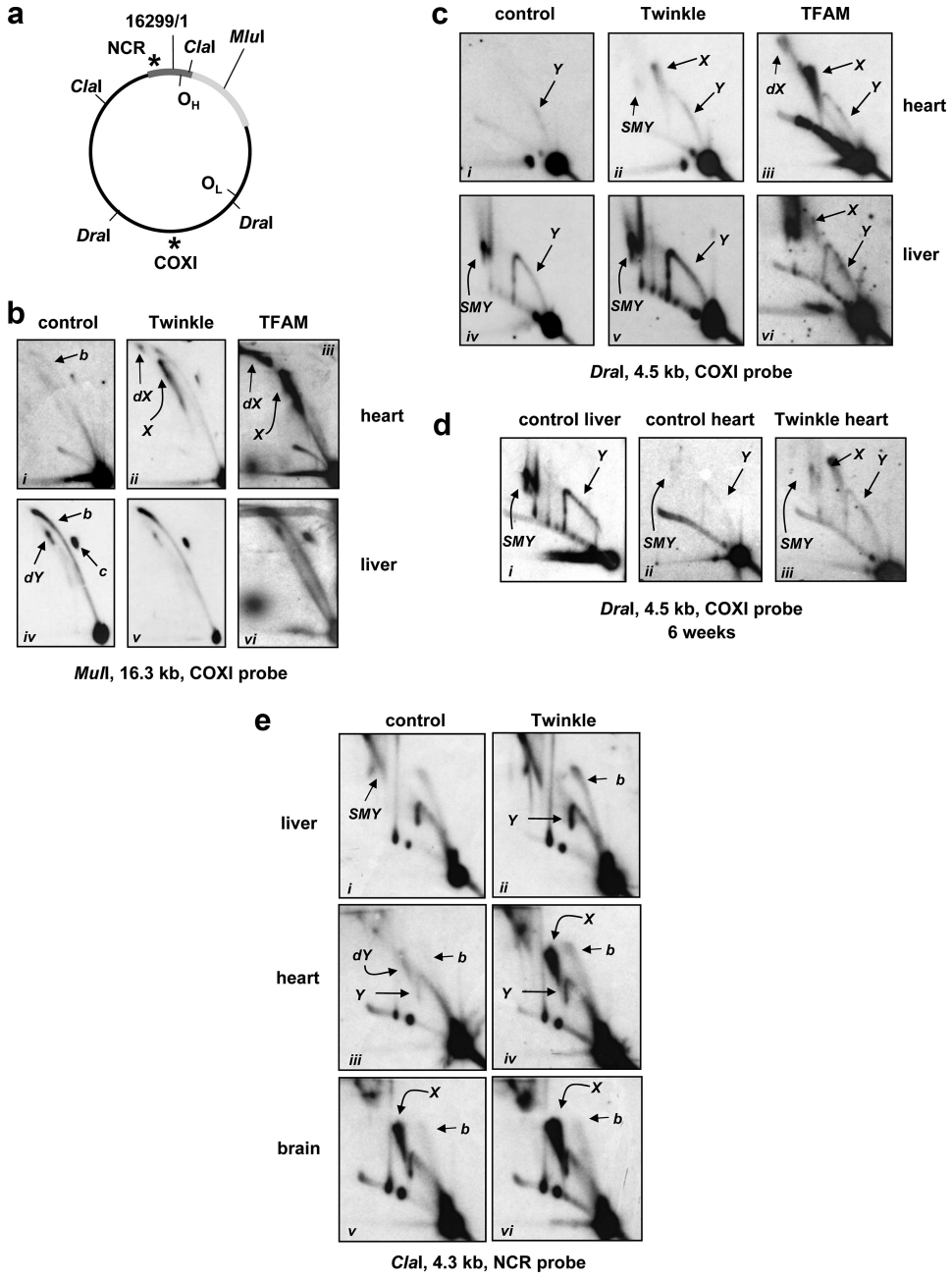

FIGURE 6. **Two-dimensional AGE analysis of mtRIs in Twinkle and TFAM transgenic mice and non-transgenic controls.** *a*, summary map of mouse mtDNA (nomenclature as in Fig. 2) showing relevant probes and restriction fragments. *b*, MluI-linearized mtDNA from 10-month-old Twinkle transgenic mice, non-transgenic littermate controls, and 8-week-old TFAM transgenic mice with tissues and probe as indicated. The various arcs represent monomeric circles (*c*), X forms (*X*), replication bubbles (*b*), double Y (*dY*) intermediates, and forms proposed to comprise three or more fragments joined by four-way junctions (*dX*). For clarity, and where obvious, these are not indicated in each individual gel panel. In the TFAM mouse samples an additional arc is seen running below the trajectory of the standard initiation arc, which probably arose by degradation of lagging strand RNA during shipment of the samples. *c*, DraI-digested mtDNA probed for the 4.5-kb COXI-containing fragment; mice, tissues, and arcs are indicated as in *b*. *Y*, standard Y arcs; *SMY*, slow moving Y-like arcs arising from restriction site blockage due to lagging strand RNA (Yang *et al.* (16)). *d*, similar DraI digests from 6-week-old mice. The mtDNA alterations in hearts of transgenic Twinkle mice are seen already in young animals. *e*, ClaI-digested mtDNA probed for the 4.3-kb NCR-containing fragment; mice, tissues, and arcs are indicated as in *a*–*e*. Note that a double Y arc is seen in non-transgenic heart DNA where it probably corresponds with termination intermediates. A much more prominent X arc is evident in Twinkle transgenic mice in both heart and brain (and also control brain), but this arc may not extend to the double-stranded DNA linear arc except in the case of Twinkle-transgenic mouse brain, suggesting that junction formation in this fragment occurs preferentially in the center of the fragment near the O_H-distal boundary of the NCR.

replicating monomers implies that heart mtDNA does not replicate in the same way as the catenated mtDNA networks of kinetoplastids (56). Resolution of these issues will require the development and validation of a satisfactory model system, *e.g.* based on metabolic labeling in organ explants or differentiating stem cells *in vitro*, as well as the identification and functional characterization of the proteins involved.

Tissue and Species Differences in mtDNA Organization and Replication—In mtDNA from cultured human cells and most tissues, standard θ replication intermediates were easily detected both by TEM and two-dimensional AGE (see also Ref. 19), whereas junctional networks appeared to be absent. In human brain, however, we observed both standard θ intermediates and junctional complexes as if material from heart and cultured cells was simply mixed together. One simple explanation for this observation would be that brain, which contains many different cell types, may simply be heterogeneous with regard to mtDNA organization and replication with some heartlike cell types and other cells of the standard type in this respect. Alternatively the two modes of mtDNA organization and replication may co-exist in the same cells. The issue will not be easily resolved because both TEM and two-dimensional AGE require significant amounts of purified material that cannot easily be obtained by microdissection.

Circular dimers and catenanes of mtDNA were observed previously in leukemic leukocytes and other cell lines (57, 58). However, *in vivo* tissues were not studied, and the forms observed were generally much less complex than we report here for human heart. Moreover no evidence of four-way junctions was found. It is an intriguing although unlikely possibility that, in granulocytic leukemias, mtDNA replication in some way mimics human heart.

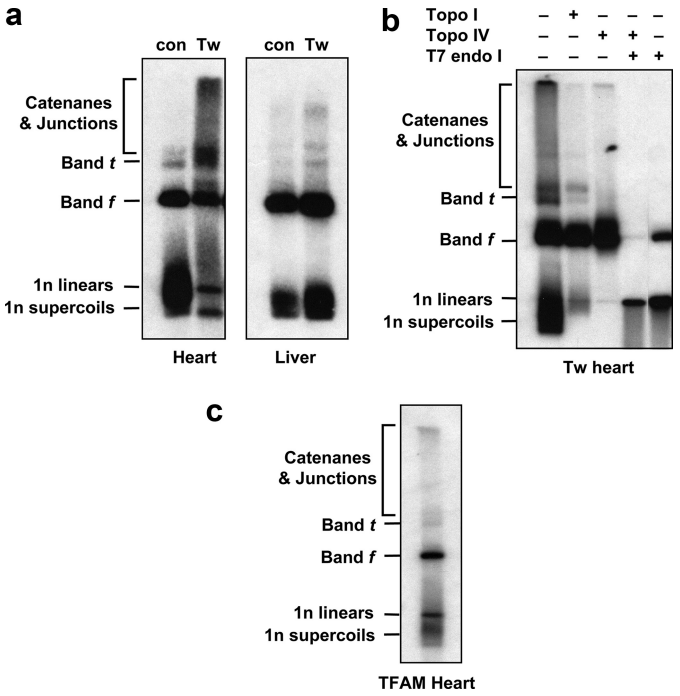

FIGURE 7. **One-dimensional AGE analysis of mtDNA in Twinkle and TFAM transgenic mice and non-transgenic controls.** *a*, one-dimensional AGE of undigested mtDNA from 10-month-old animals as indicated (*Tw*, Twinkle transgenic; *con*, non-transgenic littermate control mice). The identity of the various molecular forms is based on the enzymatic digestions of *b* plus the analysis of similar forms seen in human tissue mtDNA (Fig. 4). Bands *f* and *t* are composites of circular and junctional forms. *b*, enzymatic analysis of heart mtDNA from Twinkle transgenic mice using topoisomerases (*Topo*) I and IV and T7 endonuclease (*endo*) I as indicated. *c*, one-dimensional AGE of undigested mtDNA from 8-week-old TFAM transgenic mouse hearts. The same high molecular weight forms are seen as in Twinkle transgenic mouse hearts.

In other mammals we found an extraordinary difference from humans, namely that heart mtDNA organization and replication appeared to be of the standard θ type. In the mouse, frequent four-way junctions were found only in brain mtDNA. However, we were able to induce the formation of junctions in mouse heart mtDNA by transgenic overexpression of two different proteins implicated in mtDNA transactions, both of which also provoked an increase in mtDNA copy number (45, 59, 60). There is a rough correlation between copy number and the formation of junctional complexes. In humans, heart has the highest mtDNA copy number of any tissue studied based on our own (supplemental Table 1) as well as published measurements (61–63). However, monomeric organization is clearly not incompatible with high copy number in the case of bacterial plasmids.

In the two transgenic overexpression models we studied, TFAM had a stronger effect on both mtDNA organization and copy number than Twinkle. However, effects on mtDNA organization may be independent of those on copy number: TFAM is known to bind preferentially to four-way junctions (64), and its homologues in both bacteria (HU) and yeast mitochondria bind similarly and facilitate recombination (65–69). The viral homologue of Twinkle, the bacteriophage T7 gene 4 protein, can also catalyze directly a strand transfer reaction in the presence of the phage-encoded single-strand binding protein (70).

Another possibility is that the species differences are related only to developmental timing, *i.e.* reflecting a programmed developmental switch from standard to junctional mtDNA organization in human heart possibly connected also with aging. All human cardiac samples to which we had access were far older in years than the maximum mouse lifespan even if some were relatively young considered as a fraction of total *human* lifespan. However, there are many physiological differences between human and mouse heart (*e.g.* work load, beat rate, and reserve capacity) that could underlie the difference.

Functional Significance of Junctional mtDNA Organization—Even if they reflect high mtDNA copy number, the functional significance of junctional mtDNA networks inferred to be replicating by a non-θ mechanism is unclear. We offer two hypotheses, which future experiments in model systems may be able to address.

A high frequency of somatic recombination in a multicopy genome can be considered as one means of suppressing the sequence variation arising by somatic mutation. In effect, this provides a copy correction mechanism operating in tissues with a high metabolic rate and thus most susceptible to reactive oxygen species-induced mtDNA damage. The mouse TFAM and Twinkle models offer a potential way to test this hypothesis. Alternatively in tissues where such damage is inevitable, an mtDNA organization that keeps variant molecules physically linked may minimize segregation and thus maximize complementation. Intriguingly TFAM overexpression in mouse heart also confers resistance to the damaging effects of ischemic stress (59).

Another explanation for junctional organization would be that it facilitates high level gene expression. Although four-way junctions present a theoretical barrier to transcription, efficient branch migration and resolution may mitigate this problem. A junctional network may facilitate recycling of transcriptional complexes in a manner analogous with the transcriptional factories of the nucleolus. This may be of special importance in tissues where intracellular organization dictates that the biogenesis of new oxidative phosphorylation complexes should be spatially concentrated or restricted, *e.g.* in neuronal synapses or in the highly organized myofibrils of heart muscle.

This study constitutes the first report of tissue-specific differences in mtDNA organization and replication in mammals. Given the enormous tissue variability in the manifestations of mitochondrial disease in humans, a full understanding of this phenomenon is likely to have major implications for mitochondrial pathophysiology.

REFERENCES

1. Saccone, C. (1994) *Curr. Opin. Genet. Dev.* **4,** 875–881
2. Burger, G., Forget, L., Zhu, Y., Gray, M. W., and Lang, B. F. (2003) *Proc. Natl. Acad. Sci. U.S.A.* **100,** 892–897
3. Shapiro, T. A., and Englund, P. T. (1995) *Annu. Rev. Microbiol.* **49,** 117–143
4. Maleszka, R., Skelly, P. J., and Clark-Walker, G. D. (1991) *EMBO J.* **10,** 3923–3229
5. Han, Z., and Stachow, C. (1994) *Chromosoma* **103,** 162–170
6. Backert, S., Dörfel, P., Lurz, R., and Börner, T. (1996) *Mol. Cell. Biol.* **16,** 6285–6294
7. Preiser, P. R., Wilson, R. J., Moore, P. W., McCready, S., Hajibagheri, M. A., Blight, K. J., Strath, M., and Williamson, D. H. (1996) *EMBO J.* **15,** 684–693
8. Backert, S., and Börner, T. (2000) *Curr. Genet.* **37,** 304–314

9. Akins, R. A., Kelley, R. L., and Lambowitz, A. M. (1986) *Cell* **47,** 505–516
10. Kirschner, R. H., Wolstenholme, D. R., and Gross, N. J. (1968) *Proc. Natl. Acad. Sci. U.S.A.* **60,** 1466–1472
11. Robberson, D. L., Kasamatsu, H., and Vinograd, J. (1972) *Proc. Natl. Acad. Sci. U.S.A.* **69,** 737–741
12. Robberson, D. L., and Clayton, D. A. (1972) *Proc. Natl. Acad. Sci. U.S.A.* **69,** 3810–3814
13. Crews, S., Ojala, D., Posakony, J., Nishiguchi, J., and Attardi, G. (1979) *Nature* **277,** 192–198
14. Clayton, D. A. (1982) *Cell* **28,** 693–705
15. Holt, I. J., Lorimer, H. E., and Jacobs, H. T. (2000) *Cell* **100,** 515–524
16. Yang, M. Y., Bowmaker, M., Reyes, A., Vergani, L., Angeli, P., Gringeri, E., Jacobs, H. T., and Holt, I. J. (2002) *Cell* **111,** 495–505
17. Bowmaker, M., Yang, M. Y., Yasukawa, T., Reyes, A., Jacobs, H. T., Huberman, J. A., and Holt, I. J. (2003) *J. Biol. Chem.* **278,** 50961–50969
18. Reyes, A., Yang, M. Y., Bowmaker, M., and Holt, I. J. (2005) *J. Biol. Chem.* **280,** 3242–3250
19. Yasukawa, T., Yang, M. Y., Jacobs, H. T., and Holt, I. J. (2005) *Mol. Cell* **18,** 651–662
20. Yasukawa, T., Reyes, A., Cluett, T. J., Yang, M. Y., Bowmaker, M., Jacobs, H. T., and Holt, I. J. (2006) *EMBO J.* **25,** 5358–5371
21. Michel, B., Boubakri, H., Baharoglu, Z., LeMasson, M., and Lestini, R. (2007) *DNA Repair* **6,** 967–980
22. Fujiwara, Y., and Tatsumi, M. (1976) *Mutat. Res.* **37,** 91–110
23. Seigneur, M., Bidnenko, V., Ehrlich, S. D., and Michel, B. (1998) *Cell* **95,** 419–430
24. McGlynn, P., and Lloyd, R. G. (2002) *Nat. Rev. Mol. Cell Biol.* **3,** 859–870
25. Michel, B., Flores, M. J., Viguera, E., Grompone, G., Seigneur, M., and Bidnenko, V. (2001) *Proc. Natl. Acad. Sci. U.S.A.* **98,** 8181–8188
26. Sandler, S. J., Samra, H. S., and Clark, A. J. (1996) *Genetics* **143,** 5–13
27. Kogoma, T., Cadwell, G. W., Barnard, K. G., and Asai, T. (1996) *J. Bacteriol.* **178,** 1258–1264
28. Michel, B., Grompone, G., Florès, M. J., and Bidnenko, V. (2004) *Proc. Natl. Acad. Sci. U.S.A.* **101,** 12783–12788
29. Mosig, G. (1998) *Annu. Rev. Genet.* **32,** 379–413
30. Helleday, T. (2003) *Mutat. Res.* **532,** 103–115
31. Smith, K. C. (2004) *Bioessays* **26,** 1322–1326
32. Hinz, J. M., Tebbs, R. S., Wilson, P. F., Nham, P. B., Salazar, E. P., Nagasawa, H., Urbin, S. S., Bedford, J. S., and Thompson, L. H. (2006) *Nucleic Acids Res.* **34,** 1358–1368
33. Thompson, L. H., and Schild, D. (2002) *Mutat. Res.* **509,** 49–78
34. Barr, C. M., Neiman, M., and Taylor, D. R. (2005) *New Phytol.* **168,** 39–50
35. D'Aurelio, M., Gajewski, C. D., Lin, M. T., Mauck, W. M., Shao, L. Z., Lenaz, G., Moraes, C. T., and Manfredi, G. (2004) *Hum. Mol. Genet.* **13,** 3171–3179
36. Zsurka, G., Kraytsberg, Y., Kudina, T., Kornblum, C., Elger, C. E., Khrapko, K., and Kunz, W. S. (2005) *Nat. Genet.* **37,** 873–877
37. Holt, I. J., Dunbar, D. R., and Jacobs, H. T. (1997) *Hum. Mol. Genet.* **6,** 1251–1260
38. Tang, Y., Manfredi, G., Hirano, M., and Schon, E. A. (2000) *Mol. Biol. Cell* **11,** 2349–2358
39. Khazi, F. R., Edmondson, A. C., and Nielsen, B. L. (2003) *Mol. Genet. Genomics* **269,** 454–463
40. Odahara, M., Inouye, T., Fujita, T., Hasebe, M., and Sekine, Y. (2007) *Genes Genet. Syst.* **82,** 43–51
41. Thyagarajan, B., Padua, R. A., and Campbell, C. (1996) *J. Biol. Chem.* **271,** 27536–27543
42. Kajander, O. A., Karhunen, P. J., Holt, I. J., and Jacobs, H. T. (2001) *EMBO Rep.* **2,** 1007–1012
43. Pohjoismäki, J. L., Wanrooij, S., Hyvärinen, A. K., Goffart, S., Holt, I. J., Spelbrink, J. N., and Jacobs, H. T. (2006) *Nucleic Acids Res.* **34,** 5815–5828
44. Hyvärinen, A. K., Pohjoismäki, J. L., Reyes, A., Wanrooij, S., Yasukawa, T., Karhunen, P. J., Spelbrink, J. N., Holt, I. J., and Jacobs, H. T. (2007) *Nucleic Acids Res.* **35,** 6458–6474
45. Tyynismaa, H., Sembongi, H., Bokori-Brown, M., Granycome, C., Ashley, N., Poulton, J., Jalanko, A., Spelbrink, J. N., Holt, I. J., and Suomalainen, A. (2004) *Hum. Mol. Genet.* **13,** 3219–3227
46. Davis, R. W., and Davidson, N. (1968) *Proc. Natl. Acad. Sci. U.S.A.* **60,** 243–250
47. Thresher, R., and Griffith, J. (1992) *Methods Enzymol.* **211,** 481–490
48. Fouché, N., Ozgür, S., Roy, D., and Griffith, J. D. (2006) *Nucleic Acids Res.* **34,** 6044–6050
49. Szostak, J. W., Orr-Weaver, T. L., Rothstein, R. J., and Stahl, F. W. (1983) *Cell* **33,** 25–35
50. Ling, F., Hori, A., and Shibata, T. (2007) *Mol. Cell. Biol.* **27,** 1133–1145
51. Oldenburg, D. J., and Bendich, A. J. (2004) *J. Mol. Biol.* **335,** 953–970
52. Bendich, A. J. (1996) *J. Mol. Biol.* **255,** 564–588
53. Jacobs, M. A., Payne, S. R., and Bendich, A. J. (1996) *Curr. Genet.* **30,** 3–11
54. Oldenburg, D. J., and Bendich, A. J. (1996) *Plant Cell* **8,** 447–461
55. Oldenburg, D. J., and Bendich, A. J. (2001) *J. Mol. Biol.* **310,** 549–562
56. Drew, M. E., and Englund, P. T. (2001) *J. Cell Biol.* **153,** 735–744
57. Clayton, D. A., and Vinograd, J. (1967) *Nature* **216,** 652–657
58. Clayton, D. A., Smith, C. A., Jordan, J. M., Teplitz, M., and Vinograd, J. (1968) *Nature* **220,** 976–979
59. Ikeuchi, M., Matsusaka, H., Kang, D., Matsushima, S., Ide, T., Kubota, T., Fujiwara, T., Hamasaki, N., Takeshita, A., Sunagawa, K., and Tsutsui, H. (2005) *Circulation* **112,** 683–690
60. Ekstrand, M. I., Falkenberg, M., Rantanen, A., Park, C. B., Gaspari, M., Hultenby, K., Rustin, P., Gustafsson, C. M., and Larsson, N. G. (2004) *Hum. Mol. Genet.* **13,** 935–944
61. Barthélémy, C., Ogier de Baulny, H., Diaz, J., Cheval, M. A., Frachon, P., Romero, N., Goutieres, F., Fardeau, M., and Lombès, A. (2001) *Ann. Neurol.* **49,** 607–617
62. Miller, F. J., Rosenfeldt, F. L., Zhang, C., Linnane, A. W., and Nagley, P. (2003) *Nucleic Acids Res.* **31,** e61
63. Frahm, T., Mohamed, S. A., Bruse, P., Gemünd, C., Oehmichen, M., and Meissner, C. (2005) *Mech. Ageing Dev.* **126,** 1192–1200
64. Ohno, T., Umeda, S., Hamasaki, N., and Kang, D. (2000) *Biochem. Biophys. Res. Commun.* **271,** 492–498
65. Dri, A. M., Moreau, P. L., and Rouvière-Yaniv, J. (1992) *Gene* **120,** 11–16
66. Li, S., and Waters, R. (1998) *J. Bacteriol.* **180,** 3750–3756
67. Zelenaya-Troitskaya, O., Newman, S. M., Okamoto, K., Perlman, P. S., and Butow, R. A. (1998) *Genetics* **148,** 1763–1776
68. MacAlpine, D. M., Perlman, P. S., and Butow, R. A. (1998) *Proc. Natl. Acad. Sci. U.S.A.* **95,** 6739–6743
69. Kamashev, D., and Rouviere-Yaniv, J. (2000) *EMBO J.* **19,** 6527–6535
70. Kong, D., and Richardson, C. C. (1996) *EMBO J.* **15,** 2010–2019